Available online at www.sciencedirect.com
ScienceDirect
Journal of Molecular Spectroscopy 248 (2008) 111–121
Journal of MOLECULAR SPECTROSCOPY
www.elsevier.com/locate/jms

Radiative transition parameters for the $A^1\Sigma_u^+ - X^1\Sigma_g^+$ band system of $^{107,109}\mathrm{Ag}_2$

Russ R. Laher [a,*], Murtadha A. Khakoo [b], A. Antić-Jovanović [c]

[a] Spitzer Science Center, California Institute of Technology, M/S 314-6, Pasadena, CA 91125, USA
[b] Department of Physics, California State University Fullerton, Fullerton, CA 92834, USA
[c] Faculty of Physical Chemistry, University of Belgrade, P.O. Box 137, 1001 Belgrade, Serbia

Received 31 July 2007; in revised form 3 December 2007
Available online 28 January 2008

Abstract

Radiative transition parameters are tabulated for the $A^1\Sigma_u^+ - X^1\Sigma_g^+$ band system of the silver dimer $^{107,109}\mathrm{Ag}_2$ for bands involving vibrational levels up to $v' = 54$ and $v'' = 98$, which amply covers the band transitions empirically studied in the seminal work of Kleman and Lindkvist [B. Kleman, S. Lindkvist, Arkiv för Fysik 9 (1955) 385–390]. The tabulated parameters include band-origin wavelengths and wavenumbers, Franck–Condon factors, r-centroids, electronic transition moments, Einstein coefficients (spontaneous emission rates) and absorption band oscillator strengths. Rydberg–Klein–Rees potential energy curves for both electronic states, based on the latest available spectroscopic constants, were calculated, and then used to solve the radial Schrödinger equation for the vibrational wave functions, $\psi_{v'}$ and $\psi_{v''}$. The constant electronic transition moment function $R_e(r) = 3.05$ a.u. was fitted to previously reported relative absorption band strength measurements and the radiative lifetime of the $A^1\Sigma_u^+$ state. A numerical integration of $\int \psi_{v'}^* R_e(r) \psi_{v''}\,dr$ was performed in computing the Einstein coefficients and absorption band oscillator strengths, and these were found to differ negligibly from similar results obtained with the r-centroid approximation, as expected for a constant $R_e(r)$ function.

Keywords: Molecular bands; Absorption; Emission; Fluorescence; Band origins; Einstein coefficients; Absorption band oscillator strengths; Electronic transition moment function; Franck-Condon factors; r-centroids; Radiative transition parameters; Ag_2; Silver dimer

1. Introduction

The $A^1\Sigma_u^+ - X^1\Sigma_g^+$ band system of the $^{107,109}\mathrm{Ag}_2$ molecule has received considerable scientific interest since the 1950s. Absorption and emission $A - X$ bands from silver dimers in the vapor phase have been observed in the ≈4000 to 5200 Å range [1–7]. Given the natural abundances of silver atom isotopes, bands from $^{107,109}\mathrm{Ag}_2$ are about twice as intense as bands from the isotope molecules $^{107,107}\mathrm{Ag}_2$ and $^{109,109}\mathrm{Ag}_2$, which are typically co-produced by the experimental apparatus. Kleman and Lindkvist [1] analyzed their spectral data and published vibrational constants for the $X^1\Sigma_g^+$ ground state and the $A^1\Sigma_u^+$ lowest-excited state of the $^{107,109}\mathrm{Ag}_2$ molecule. Their vibrational constants are based on measured transitions involving vibrational levels as high as $v' = 33$ for the A state and $v'' = 45$ for the X state (the primed symbols denote upper states and the double-primed symbols denote lower states). Since that landmark paper, only scant work has been done to verify these vibrational constants [5,7].

In the 1990s, high-resolution laser spectroscopy allowed the rotational structure of the $A - X$ bands to be probed [8–10]. However, only bands with low vibrational levels were analyzed. For example, Beutel et al. [8] determined rotational constants for both X and A states from measurements of three absorption bands: $(v' = 1, v'' = 0)$, $(v' = 2, v'' = 0)$, and $(v' = 1, v'' = 1)$. Around the same time, Simard et al. [9] performed a rotational analysis and obtained similar results to within a few percent or better.

There are some reported measurements of Einstein coefficients and radiative lifetimes for the A state of the

---

[*] Corresponding author. Fax: +1 626 568 0673.
E-mail address: laher@ipac.caltech.edu (R.R. Laher).

0022-2852/$ - see front matter © 2007 Elsevier Inc. All rights reserved.
doi:10.1016/j.jms.2007.12.003

Ag_2 molecule in the literature, but it is not obvious to which vibrational levels the measurements apply (if they can indeed be separated). Hebert et al. [11] obtained an Einstein coefficient of 3.7×10^8 s^{-1}, the inverse of which corresponds to a radiative lifetime of 2.7 ns. In later work, Hebert et al. [12] took the lifetime of the $A-X$ emission to be 3.5 ns, citing their previous paper. König et al. [13] determined a lifetime of 4.6 ns, and later König's coauthors [14] reinforced this result in discussing their study of light emission from silver clusters in noble gas matrices. The assignment of these measurements to specific vibrational levels is not important for our purposes, because all the lower levels have nearly the same radiative lifetimes, as shown below.

Recently, Antić-Jovanović et al. [2] measured the relative strengths of several $^{107,109}Ag_2$ $A-X$ absorption bands and compared ratios of their measurements with ratios of calculated relative absorption band strengths, obtaining agreement to within ±8%. This is an important development because relative absorption band strength measurements and Franck–Condon factors were heretofore unavailable for this band system. Prior to this, one could only infer strong bands by their presence in published band-head tables, and weak bands by those that were missing from the tables.

In the present work, we assumed constant and linear models for the electronic transition moment function as a function of internuclear distance and performed data fits to the empirical data of Antić-Jovanović et al. [2]. We determined the best model and were then able to normalize our electronic transition moment function to absolute data units with the measured radiative lifetime. This put us in the position of being able to compute Einstein coefficients (spontaneous emission rates) and absorption band oscillator strengths for individual bands in the $A-X$ system, thus making the picture more complete for spectroscopists and future work. Herein, we report a complete set of calculated band-origin wavelengths and wavenumbers, Franck–Condon factors, r-centroids, Einstein coefficients and absorption band oscillator strengths for the $A-X$ band system of the $^{107,109}Ag_2$ isotopomer.

2. Methods

The relative absorption strength (measured signal), $I_{v'v''}$, produced by the $v' \leftarrow v''$ band transition is proportional to the product of three terms (e.g., see [2]):

$$I_{v'v''} \propto N_{v''} \nu_{v'v''} p_{v'v''}, \tag{1}$$

where $N_{v''}$ is the population of the v'' level, $\nu_{v'v''}$ is the band-origin wavenumber of the transition and $p_{v'v''}$ is defined as

$$p_{v'v''} \equiv [\langle \psi_{v'}(r) | R_e(r) | \psi_{v''}(r) \rangle]^2. \tag{2}$$

Eq. (2) is the dominant contributor to the variation of vibrational band strengths in electronic vibrational–rotational transitions. The wave functions, $\psi_{v'}(r)$ and $\psi_{v''}(r)$, correspond to the rotationless ($J = 0$) vibrational levels in the upper and lower electronic states, respectively, and $R_e(r)$ is the electronic transition moment function (ETMF), which is commonly represented as a function of internuclear distance, r. For many band systems, $R_e(r)$ can be well approximated by a constant or a linear function of r, at least in regions where the integrand in Eq. (2) is appreciable. In this case, the r-centroid approximation can be employed [15–17], and Eq. (2) becomes

$$p_{v'v''} \approx [\langle \psi_{v'}(r) | \psi_{v''}(r) \rangle]^2 R_e^2(\bar{r}_{v'v''}). \tag{3}$$

The first term in this equation is the square of overlap integral or Franck–Condon factor (FCF), $q_{v'v''}$, and the function argument in the second term is the weighted mean of the internuclear distance or r-centroid, $\bar{r}_{v'v''}$, for the (v', v'') band:

$$q_{v'v''} \equiv [\langle \psi_{v'}(r) | \psi_{v''}(r) \rangle]^2 \tag{4}$$

and

$$\bar{r}_{v'v''} \equiv \frac{\langle \psi_{v'}(r) | r | \psi_{v''}(r) \rangle}{\langle \psi_{v'}(r) | \psi_{v''}(r) \rangle}. \tag{5}$$

The calculation of $p_{v'v''}$ in the r-centroid approximation, therefore, depends on the determination of both the FCF, which is calculated from the vibrational wavefunctions, and $R_e(r)$, which can be obtained either by an *ab initio* calculation or derived from spectroscopic band strength measurements. In our study, we have applied the latter method for estimating $R_e(r)$.

The accuracy of the calculated $q_{v'v''}$ and $\bar{r}_{v'v''}$ values depends on knowledge of the potential energy curves of the lower and upper electronic states, which are used in the radial Schrödinger equation to solve for the rotationless vibrational wavefunctions $\psi_{v'}(r)$ and $\psi_{v''}(r)$. We computed RKR (Rydberg–Klein–Rees) potential energy curves using the spectroscopic constants given in Table 1. In order to derive dissociation limits for the potential energy curves, we reasonably assumed that the dissociation energy of the X state corresponds to the Ag atoms separating in the ground state ($\mathrm{Ag\,4d^{10}5s\,^2S_{1/2}} + \mathrm{Ag\,4d^{10}5s\,^2S_{1/2}}$),

Table 1
Spectroscopic constants of the $X^1\Sigma_g^+$ and $A^1\Sigma_u^+$ states of $^{107,109}Ag_2$

Constant[a]	$X^1\Sigma_g^+$	$A^1\Sigma_u^+$	Ref.
T_e	−96.039	22899.677	[1]
T_0	0[b]	22976.831[c]	
ω_e	192.4	154.6	[1]
$\omega_e x_e$	0.643	0.587	[1]
$\omega_e y_e$	0.0003	0.0022[d]	[1]
B_e	0.048807(5)	0.044354(5)	[8]
α_e	$2.08(3) \times 10^{-4}$	$2.19(3) \times 10^{-4}$	[8]
r_e (Å)	2.53	2.65	See text
Dissoc. energy	13,308[e]	19,882[f]	

[a] All values are in data units of cm^{-1}, unless otherwise noted.

[b] Adjusted T_e of the X state to give $T_0 = 0\ cm^{-1}$, as is now customary.

[c] Adjusted T_e of the A state to give the corresponding ν_{00} value of [9].

[d] Note that [18] has a typographical error in the last digit for this constant.

[e] This is the dissociation energy of 1.65 eV as cited by [19], which is relative to the $v'' = 0$ term value of the X state, and corresponds to $\mathrm{Ag\,4d^{10}5s\,^2S_{1/2}} + \mathrm{Ag\,4d^{10}5s\,^2S_{1/2}}$.

[f] Computed relative to the $v' = 0$ term value of the A state, and corresponds to $\mathrm{Ag\,4d^{10}5s\,^2S_{1/2}} + \mathrm{Ag\,4d^{10}5p\,^2P^o_{1/2}}$.

and the dissociation energy of the A state corresponds to separation between one Ag atom in the ground state and the other Ag atom in the lowest excited state ($\mathrm{Ag}\,4\mathrm{d}^{10}5\mathrm{s}^2S_{1/2} + \mathrm{Ag}\,4\mathrm{d}^{10}5\mathrm{p}^2P^o_{1/2}$); this is consistent with Ruamps [3] and past theoretical work [19,20].

In order to derive the ETMF, we separately fitted a constant function [$R_e(r) = \mathrm{const.}$] and a linear function [$R_\mathrm{e}(\bar{r}_{v'v''}) = a + b\bar{r}_{v'v''}$] to the measured ratios of absorption strengths for the various $^{107,109}\mathrm{Ag}_2\ A-X$ bands observed by Antić-Jovanović et al. [2]. In the latter case, the standard assumption that the ETMF depends parametrically on the r-centroid, $\bar{r}_{v'v''}$, was invoked (see Fraser [17]). We set up our calculations to minimize the root mean-squared error (R.M.S.E.) between the measurements and our computed absorption band oscillator strengths. We also included in the calculations the constraint that the inverse of the sum of our computed Einstein coefficients over $0 \leqslant v'' \leqslant 98$ for $v' = 0$ is to equal the measured $^{107,109}\mathrm{Ag}_2 A^1\Sigma_u^+$-state radiative lifetime of 4.6 ns [13]. Since the linear function did not result in a smaller R.M.S.E. value than the constant function, after taking into account the additional degree of freedom of the linear function, we had no choice but to select the constant function as the best model for the data.

Using our derived potential energy curves and ETMF, we computed a matrix of radiative transition parameters for the $^{107,109}\mathrm{Ag}_2 A^1\Sigma_u^+ - X^1\Sigma_g^+$ band system, for $v'' \leqslant 98$ and $v' \leqslant 54$, with the computer program of Espy [21]. Our calculations included numerically integrating Eq. (2), which was subsequently used to compute Einstein coefficients, $A_{v'v''}$, and absorption band oscillator strengths, $f^\mathrm{abs}_{v'v''}$, from the following well known formulas (e.g., [21–24]):

$$A_{v'v''} = \frac{16\pi^3 a_0^2 e^2 v_{v'v''}^3 (2-\delta_{0,\Lambda'+\Lambda''})}{3h\epsilon_0(2-\delta_{0,\Lambda'})} p_{v'v''} \approx 2.026\times10^{-6} v_{v'v''}^3 \frac{(2-\delta_{0,\Lambda'+\Lambda''})}{(2-\delta_{0,\Lambda'})} \times [\langle\psi_{v'}(r)|R_\mathrm{e}(r)|\psi_{v''}(r)\rangle]^2, \tag{6}$$

$$f^\mathrm{abs}_{v'v''} = \frac{8\pi^2 m_\mathrm{e} c a_0^2 v_{v'v''}(2-\delta_{0,\Lambda'+\Lambda''})}{3h(2-\delta_{0,\Lambda'})} p_{v'v''} \approx 3.0376\times10^{-6} v_{v'v''} \frac{(2-\delta_{0,\Lambda'+\Lambda''})}{(2-\delta_{0,\Lambda'})} \times [\langle\psi_{v'}(r)|R_\mathrm{e}(r)|\psi_{v''}(r)\rangle]^2. \tag{7}$$

Here, an electronic-vibrational band transition is represented by $^{2S'+1}\Lambda'(v') \to {}^{2S''+1}\Lambda''(v'')$, where S is the total electronic spin quantum number and Λ is the quantum number of the component of the total electronic angular momentum along the internuclear axis, which takes on values 0, 1, 2, ... corresponding to the electronic state symbols Σ, Π, Δ, ... For the A and X states, $S' = S'' = 0$ and $\Lambda' = \Lambda'' = 0$. Eqs. (6) and (7) are valid for spin-allowed transitions, i.e., with $S' = S''$. In these equations, the band-origin wavenumber of the transition, $v_{v'v''}$, is in units of cm^{-1}, $R_\mathrm{e}(r)$ is in electric dipole moment atomic units (a.u.), $A_{v'v''}$ is in units of s^{-1}, $f^\mathrm{abs}_{v'v''}$ is dimensionless, and $\delta_{0,\Lambda}$ is the Kronecker delta, which equals 1 if $\Lambda = 0$ and zero otherwise. The remaining terms in the first part of each of these equations are defined in Appendix A.

The computer program also includes a parallel calculation of Eq. (3), for comparison of results as a test of the r-centroid approximation.

3. Results

Fig. 1 shows our computed RKR potential energy curves for the $X^1\Sigma_g^+$ and $A^1\Sigma_u^+$ states of the $^{107,109}\mathrm{Ag}_2$ molecule. Our curves differ somewhat from those of Beutel et al. [25] in the details at the lower range of internuclear distances shown and near the regions of equilibrium internuclear distance. The former is not surprising because the extrapolation of the curves to small internuclear distances is sensitive to the maximum vibrational level specified for the calculation. At the higher range of internuclear distances, however, our dissociation limits for the X and A states are the same as theirs. Our curve for the X state has a slight kink at ≈2.10 Å, which is an artifact of the extrapolation based on a Morse-type function to a region where the wavefunction becomes small and, therefore, has negligible effect on the calculations [21].

Using the method discussed in the previous section, our ETMF result is

$$R_\mathrm{e}(r) = 3.05\ \mathrm{a.u.}, \tag{8}$$

where $R_\mathrm{e}(r)$ is in electric dipole moment atomic units (a.u.) and independent of r-centroid. We caution the reader that this function has been validated only over the 2.46–2.81 Å range of internuclear distances.

Fig. 2 is a scatter plot of the strongest $^{107,109}\mathrm{Ag}_2\ A-X$ bands from our calculations, i.e., those with Einstein coefficients $\geqslant 10^7\ \mathrm{s}^{-1}$. The data outline an open, symmetric Franck–Condon envelope with a truncated upper leg, relatively sharp outside edges, and a scattering of strong bands

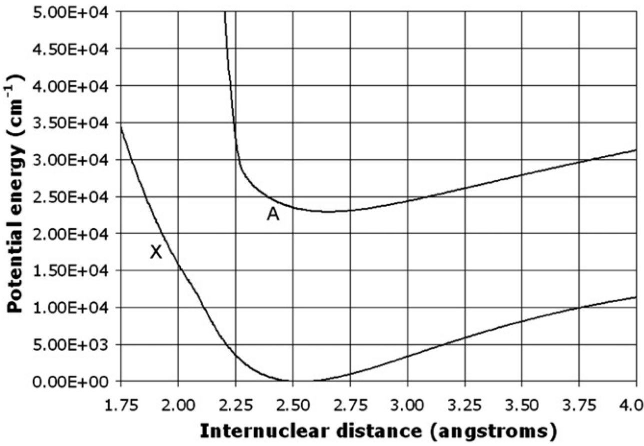

Fig. 1. RKR potential energy curves for the $X^1\Sigma_g^+$ and $A^1\Sigma_u^+$ states of the $^{107,109}\mathrm{Ag}_2$ molecule, calculated from the data of Table 1. The slight dip of the curve for the X state below the abscissa's axis is because a term value of zero for $v'' = 0$ has been defined in this work.

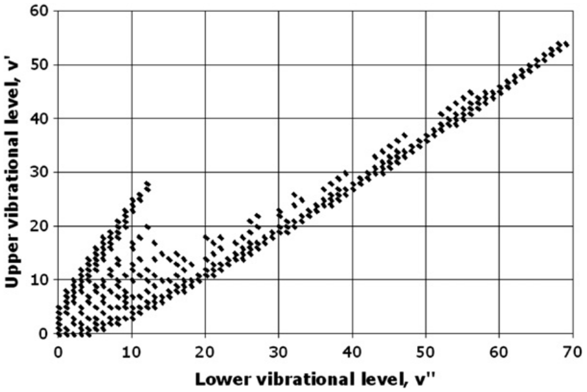

Fig. 2. Scatter plot of $^{107,109}\mathrm{Ag}_2 A^1\Sigma_u^+ - X^1\Sigma_g^+$ $(v' - v'')$ bands with Einstein coefficients $\geqslant 10^7$ s^{-1}.

in its interior near the apex and along the lower leg. Our calculations covered $0 \leqslant v'' \leqslant 98$ and $0 \leqslant v' \leqslant 54$, and the upper ranges of these vibrational numbers are near the dissociation limits and just below where the calculations break down for the two electronic states.

Tables 2 and 3 present a partial set of our calculated radiative transition parameters for the $^{107,109}\mathrm{Ag}_2 A^1\Sigma_u^+ - X^1\Sigma_g^+$ band system, covering $0 \leqslant v' \leqslant 13$ and $0 \leqslant v'' \leqslant 19$, which encompasses about half of the bands reported on by Kleman and Lindkvist [1]. For each $v' - v''$ band, the listed quantities are $\lambda_{v'v''}$ (μm), $\nu_{v'v''}$ (cm^{-1}), $q_{v'v''}$ (Franck–Condon factor), $\bar{r}_{v'v''}$ (r-centroid, in Å), $A_{v'v''}$ (spontaneous emission rate, in s^{-1}), and $f^{\mathrm{abs}}_{v'v''}$ (absorption band oscillator strength).

Table 4 gives radiative transition parameters for selected bands of the $A^1\Sigma_u^+ - X^1\Sigma_g^+$ band system of $^{107,109}\mathrm{Ag}_2$. This table covers all the $^{107,109}\mathrm{Ag}_2$ bands listed by Kleman and Lindkvist [1] in their Table 1. The calculations were done with our derived constant electronic transition moment function $R_e(r) = 3.05$ a.u. Except for the 0–6 band, which may have been misidentified (the spectral feature assigned to the 0–6 band could easily be reassigned to the 6–11 band, which lies in the adjacent $\Delta v = -5$ sequence and is more than four times stronger than the 0–6 band, according to our calculations), all bands in this table have Franck–Condon factors greater than 0.01.

4. Discussion

The resulting equilibrium internuclear distances associated with our RKR potential energy curves exactly match the values independently reported by Simard et al. [9] and six months later by Krämer et al. [10], which are 2.53 and 2.65 Å for the X and A states, respectively. According to Beutel et al. [25], the r_e value for the X state is markedly larger than the value of 2.469 Å computed by Brown and Ginter [5] from interpolation of Cu_2 and Au_2 data with the Morse–Clark formula [26]; this demonstrates the limitation of this approximate method, as well as its utility.

Fig. 3 shows the calculated radiative lifetime of the $^{107,109}\mathrm{Ag}_2 A^1\Sigma_u^+$ state as a function of vibrational level, v. We computed these results by summing the Einstein coefficients over v'' for each A-state vibrational level, and then taking the inverse of the resulting sum. There is only a ≈20% variation between the lowest and highest states treated, which is probably less than the uncertainty of the measured lifetimes.

Kleman and Lindkvist [1] reported band-head wavenumbers for a small portion of the strong $^{107,109}\mathrm{Ag}_2 A^1\Sigma_u^+ - X^1\Sigma_g^+$ bands that we found from our calculations, for up to $v' = 33$ and $v'' = 45$. These bands tend to lie along the sharp bottom edge of the Franck–Condon envelope (see Fig. 2). Our tabulated results show a number of cases of unreported strong bands with the same v' or v'' as the reported bands. For example, Kleman and Lindkvist list band-head wavenumbers for the $(v' = 26, v'' = 38)$ and $(v' = 27, v'' = 38)$ bands, but not the similarly strong $(v' = 25, v'' = 38)$, $(v' = 27, v'' = 36)$, and $(v' = 27, v'' = 40)$ bands. It would be interesting to examine a few of these cases in the laboratory with modern equipment, and confirm both calculated band origins and strengths.

The Franck–Condon factors sum to unity across v'' for each v' covered by our radiative-transition-parameter tables, i.e., up to $v' = 54$. In the other dimension, summing over v' for a given v'' yields unity for all $v'' \leqslant 12$; the separate sums over v' for a given v'' where $v'' > 12$ is less than unity, progressively decreases as v'' increases, and reaches zero at $v'' = 73$.

As expected for the constant $R_e(r)$ function given by Eq. (8), we found negligible differences between Einstein coefficients calculated by numerical integration of $\int \psi^*_{v'} R_e(r) \psi_{v''}\, dr$ versus by the r-centroid approximation for the $^{107,109}\mathrm{Ag}_2 A^1\Sigma_u^+ - X^1\Sigma_g^+$ band system.

In general, the accuracy of our results will be degraded at the higher vibrational levels, where the corresponding spectral data are sparse or not available for deriving higher-order vibrational and rotational constants than were used in this work. We also attribute lower accuracy to bands lying outside of the applicable range of our ETMF.

There is good agreement between the experimental measurements of relative absorption band strengths and our theoretical results, since this is enforced by our ETMF data fit. The match is to within ±8%, which is approximately the same as the previous match to calculated relative absorption band strengths (see [2]). This error is consistent with our finding that the ETMF has no discernible dependence on internuclear distance.

We have restricted the range of vibrational levels published in this paper to reduce the number of pages, but our complete set of tables is available from the authors upon request. Besides annoying some readers with the large number of tables, there are many other good reasons for skepticism over the accuracy of the numerical results for high vibrational levels, and we are indebted to Dr. Forrest R. Gilmore for pointing these out. Applications of this band system involve hot silver vapor, in which cases our results for $J = 0$ become less applicable, since at higher v

Table 2
Radiative transition parameters for the $A^1\Sigma_u^+ - X^1\Sigma_g^+$ band system of ^{107,109}Ag$_2$

v'	$v'' = 0$	1	2	3	4	5	6	7	8	9
0	0.4352	0.4389	0.4426	0.4463	0.4500	0.4538	0.4577	0.4616	0.4655	0.4694
	22976.8	22785.7	22595.9	22407.3	22220.1	22034.1	21849.4	21665.9	21483.8	21302.9
	1.18E−01	2.70E−01	2.89E−01	1.92E−01	8.94E−02	3.09E−02	8.26E−03	1.74E−03	2.96E−04	4.08E−05
	2.5924	2.6247	2.6579	2.6919	2.7268	2.7628	2.7998	2.8381	2.8778	2.9189
	2.71E+07	6.02E+07	6.28E+07	4.07E+07	1.85E+07	6.24E+06	1.62E+06*	3.34E+05*	5.53E+04*	7.44E+03*
	7.68E−02	1.74E−01	1.84E−01	1.22E−01	5.62E−02	1.93E−02	5.10E−03*	1.07E−03*	1.80E−04*	2.46E−05*
1	0.4323	0.4359	0.4396	0.4432	0.4470	0.4507	0.4545	0.4583	0.4622	0.4661
	23130.3	22939.2	22749.3	22560.8	22373.5	22187.5	22002.8	21819.4	21637.2	21456.3
	2.32E−01	1.52E−01	6.94E−04	9.53E−02	2.06E−01	1.77E−01	9.25E−02	3.35E−02	9.01E−03	1.87E−03
	2.5664	2.5973	2.6076	2.6659	2.6991	2.7337	2.7695	2.8064	2.8446	2.8843
	5.42E+07	3.45E+07	1.54E+05*	2.06E+07	4.34E+07	3.65E+07	1.86E+07	6.56E+06	1.72E+06*	3.48E+05*
	1.52E−01	9.82E−02	4.46E−04*	6.07E−02	1.30E−01	1.11E−01	5.75E−02	2.07E−02	5.51E−03*	1.13E−03*
2	0.4295	0.4331	0.4367	0.4403	0.4439	0.4476	0.4514	0.4551	0.4589	0.4628
	23282.6	23091.4	22901.6	22713.1	22525.8	22339.8	22155.1	21971.6	21789.5	21608.6
	2.45E−01	5.74E−03	1.12E−01	1.04E−01	6.04E−05	8.99E−02	1.83E−01	1.51E−01	7.49E−02	2.56E−02
	2.5412	2.5650	2.6054	2.6360	2.5742	2.7070	2.7408	2.7763	2.8131	2.8513
	5.83E+07	1.33E+06*	2.54E+07	2.29E+07	1.30E+04*	1.89E+07	3.76E+07	3.02E+07	1.46E+07	4.87E+06
	1.61E−01	3.75E−03*	7.26E−02	6.66E−02	3.85E−05*	5.68E−02	1.15E−01	9.39E−02	4.61E−02	1.56E−02
3	0.4267	0.4302	0.4338	0.4374	0.4410	0.4446	0.4483	0.4520	0.4558	0.4596
	23433.7	23242.6	23052.7	22864.2	22676.9	22490.9	22306.2	22122.8	21940.6	21759.7
	1.86E−01	3.90E−02	1.11E−01	2.60E−03	1.16E−01	5.60E−02	7.14E−03	1.17E−01	1.72E−01	1.20E−01
	2.5168	2.5503	2.5781	2.6245	2.6441	2.6746	2.7216	2.7483	2.7833	2.8199
	4.50E+07	9.23E+06	2.57E+07	5.86E+05*	2.54E+07	1.20E+07	1.49E+06*	2.39E+07	3.43E+07	2.34E+07
	1.23E−01	2.56E−02	7.26E−02	1.68E−03*	7.41E−02	3.56E−02	4.50E−03*	7.31E−02	1.07E−01	7.40E−02
4	0.4240	0.4275	0.4310	0.4345	0.4381	0.4417	0.4453	0.4490	0.4527	0.4564
	23583.7	23392.6	23202.8	23014.2	22826.9	22640.9	22456.2	22272.8	22090.6	21909.7
	1.13E−01	1.20E−01	1.45E−02	9.16E−02	3.69E−02	3.67E−02	1.07E−01	1.31E−02	3.94E−02	1.47E−01
	2.4931	2.5245	2.5490	2.5863	2.6141	2.6535	2.6830	2.7103	2.7575	2.7905
	2.79E+07	2.89E+07	3.41E+06	2.10E+07	8.28E+06	8.02E+06	2.28E+07	2.73E+06	8.01E+06	2.91E+07
	7.53E−02	7.92E−02	9.49E−03	5.96E−02	2.38E−02	2.35E−02	6.77E−02	8.26E−03	2.46E−02	9.09E−02
5	0.4214	0.4248	0.4282	0.4317	0.4352	0.4388	0.4424	0.4460	0.4496	0.4533
	23732.6	23541.5	23351.7	23163.1	22975.8	22789.8	22605.1	22421.7	22239.5	22058.6
	5.90E−02	1.44E−01	1.34E−02	8.31E−02	1.51E−02	8.95E−02	4.97E−05	8.52E−02	6.30E−02	1.32E−03
	2.4701	2.5004	2.5356	2.5595	2.5974	2.6231	2.5339	2.6911	2.7218	2.7879
	1.49E+07	3.55E+07	3.23E+06	1.95E+07	3.45E+06	2.00E+07	1.08E+04*	1.81E+07	1.31E+07	2.67E+05*
	3.96E−02	9.61E−02	8.87E−03	5.44E−02	9.81E−03	5.77E−02	3.18E−05*	5.40E−02	3.96E−02	8.21E−04*
6	0.4188	0.4221	0.4255	0.4290	0.4325	0.4360	0.4395	0.4431	0.4467	0.4503
	23880.4	23689.3	23499.5	23310.9	23123.6	22937.6	22752.9	22569.5	22387.3	22206.4
	2.74E−02	1.17E−01	7.47E−02	1.19E−02	8.46E−02	6.03E−03	7.39E−02	3.01E−02	3.08E−02	9.45E−02
	2.4478	2.4773	2.5084	2.5304	2.5677	2.5885	2.6314	2.6586	2.7008	2.7301
	7.05E+06	2.93E+07	1.83E+07	2.84E+06	1.97E+07	1.37E+06*	1.64E+07	6.52E+06	6.51E+06	1.95E+07
	1.85E−02	7.84E−02	4.96E−02	7.83E−03	5.53E−02	3.91E−03*	4.75E−02	1.92E−02	1.95E−02	5.93E−02
7	0.4162	0.4195	0.4229	0.4263	0.4297	0.4332	0.4367	0.4402	0.4438	0.4474
	24027.1	23836.0	23646.2	23457.6	23270.3	23084.4	22899.7	22716.2	22534.0	22353.1
	1.17E−02	7.52E−02	1.12E−01	8.93E−03	6.14E−02	3.20E−02	4.81E−02	2.41E−02	7.03E−02	6.91E−04
	2.4262	2.4549	2.4848	2.5209	2.5415	2.5769	2.6024	2.6414	2.6679	2.7409
	3.06E+06	1.92E+07	2.78E+07	2.17E+06*	1.46E+07	7.42E+06	1.09E+07	5.31E+06	1.52E+07	1.45E+05*
	7.95E−03	5.06E−02	7.46E−02	5.92E−03*	4.03E−02	2.09E−02	3.11E−02	1.54E−02	4.48E−02	4.36E−04*
8	0.4137	0.4170	0.4203	0.4237	0.4271	0.4305	0.4339	0.4374	0.4409	0.4445
	24172.7	23981.6	23791.8	23603.2	23416.0	23230.0	23045.3	22861.8	22679.7	22498.8
	4.67E−03	4.13E−02	1.05E−01	5.69E−02	6.86E−03	7.71E−02	4.28E−04	7.31E−02	2.55E−05	7.47E−02
	2.4053	2.4333	2.4622	2.4930	2.5108	2.5497	2.6185	2.6110	2.8241	2.6762
	1.24E+06*	1.07E+07	2.66E+07	1.41E+07	1.66E+06*	1.82E+07	9.87E+04*	1.65E+07	5.60E+03*	1.60E+07
	3.19E−03*	2.80E−02	7.04E−02	3.79E−02	4.54E−03*	5.06E−02	2.79E−04*	4.72E−02	1.63E−05*	4.75E−02
9	0.4112	0.4145	0.4178	0.4211	0.4244	0.4278	0.4312	0.4347	0.4381	0.4416
	24317.3	24126.2	23936.4	23747.8	23560.6	23374.6	23189.9	23006.4	22824.2	22643.3
	1.77E−03	2.02E−02	7.55E−02	9.17E−02	9.04E−03	4.33E−02	4.66E−02	1.56E−02	5.54E−02	1.70E−02
	2.3852	2.4124	2.4405	2.4698	2.5056	2.5238	2.5582	2.5808	2.6194	2.6433

(*continued on next page*)

Table 2 (*continued*)

v'	$v'' = 0$	1	2	3	4	5	6	7	8	9
	4.79E+05*	5.35E+06	1.95E+07	2.31E+07	2.23E+06*	1.04E+07	1.09E+07	3.57E+06	1.24E+07	3.73E+06
	1.21E−03*	1.38E−02	5.11E−02	6.15E−02	6.02E−03*	2.86E−02	3.05E−02	1.01E−02	3.58E−02	1.09E−02
10	0.4088	0.4120	0.4153	0.4186	0.4219	0.4252	0.4286	0.4320	0.4354	0.4388
	24460.8	24269.7	24079.9	23891.3	23704.1	23518.1	23333.4	23149.9	22967.8	22786.9
	6.43E−04	9.11E−03	4.59E−02	9.20E−02	4.92E−02	2.77E−03	6.67E−02	9.73E−03	4.80E−02	1.96E−02
	2.3658	2.3922	2.4195	2.4479	2.4783	2.4878	2.5323	2.5701	2.5912	2.6297
	1.77E+05*	2.45E+06*	1.21E+07	2.36E+07	1.24E+07	6.79E+05*	1.60E+07	2.27E+06*	1.10E+07	4.38E+06
	4.45E−04*	6.25E−03*	3.12E−02	6.21E−02	3.30E−02	1.84E−03*	4.40E−02	6.36E−03*	3.12E−02	1.26E−02
11	0.4064	0.4096	0.4128	0.4161	0.4193	0.4226	0.4260	0.4293	0.4327	0.4361
	24603.3	24412.2	24222.4	24033.8	23846.6	23660.6	23475.9	23292.4	23110.3	22929.4
	2.28E−04	3.86E−03	2.47E−02	7.09E−02	7.90E−02	1.08E−02	2.86E−02	5.50E−02	1.09E−03	6.11E−02
	2.3473	2.3728	2.3993	2.4268	2.4556	2.4904	2.5064	2.5406	2.5446	2.5996
	6.39E+04*	1.06E+06*	6.61E+06	1.86E+07	2.02E+07	2.69E+06	6.97E+06	1.31E+07	2.52E+05*	1.39E+07
	1.58E−04*	2.66E−03*	1.69E−02	4.82E−02	5.33E−02	7.21E−03	1.90E−02	3.62E−02	7.09E−04*	3.96E−02
12	0.4041	0.4073	0.4104	0.4136	0.4169	0.4201	0.4234	0.4267	0.4301	0.4334
	24744.8	24553.7	24363.8	24175.3	23988.0	23802.0	23617.3	23433.9	23251.7	23070.8
	7.90E−05	1.56E−03	1.21E−02	4.60E−02	8.13E−02	4.56E−02	5.12E−04	5.42E−02	2.39E−02	2.08E−02
	2.3299	2.3543	2.3799	2.4065	2.4343	2.4641	2.4466	2.5154	2.5499	2.5711
	2.26E+04*	4.34E+05*	3.31E+06	1.23E+07	2.12E+07	1.16E+07	1.27E+05*	1.31E+07	5.67E+06	4.82E+06
	5.53E−05*	1.08E−03*	8.36E−03	3.14E−02	5.51E−02	3.07E−02	3.42E−04*	3.59E−02	1.57E−02	1.36E−02
13	0.4018	0.4050	0.4081	0.4113	0.4144	0.4177	0.4209	0.4242	0.4275	0.4308
	24885.2	24694.1	24504.3	24315.8	24128.5	23942.5	23757.8	23574.3	23392.2	23211.3
	2.72E−05	6.08E−04	5.59E−03	2.65E−02	6.51E−02	7.03E−02	1.32E−02	1.73E−02	5.64E−02	2.10E−03
	2.3135	2.3367	2.3612	2.3870	2.4138	2.4421	2.4757	2.4887	2.5237	2.5700
	7.89E+03*	1.73E+05*	1.55E+06*	7.17E+06	1.72E+07	1.82E+07	3.34E+06	4.27E+06	1.36E+07	4.95E+05*
	1.91E−05*	4.24E−04*	3.87E−03*	1.82E−02	4.44E−02	4.76E−02	8.87E−03	1.15E−02	3.73E−02	1.38E−03*

For each $v' - v''$ band, the listed quantities are $\lambda_{v'v''}$ (μm), $\nu_{v'v''}$ (cm^{-1}), $q_{v'v''}$, $\bar{r}_{v'v''}$ (Å), $A_{v'v''}$ (spontaneous emission rate, in s^{-1}), and $f^{\mathrm{abs}}_{v'v''}$ (absorption band oscillator strength). Values of $A_{v'v''}$ and $f^{\mathrm{abs}}_{v'v''}$ having a corresponding value of $q_{v'v''} < 0.01$ are marked with an asterisk to indicate possible lower accuracy.

values the results become more sensitive to the J value. At higher v values, the results (even for $J = 0$) become more uncertain because of uncertainties in the rotational constants, as we have already pointed out. Our results apply only for the major isotope and, although the combined emission from the two minor isotopes is generally about equal to that from the major isotope and the Franck–Condon factors of the various isotopes are quite similar at low v, this may be less true for higher v. Finally, at high v values, the A state curves may run into perturbations from other high states (see [20]). Nevertheless, our calculations show that the strong bands are indeed the ones that were observed by Kleman and Lindkvist [1] at fairly high vibrational levels.

5. Conclusions

In this paper, we have assembled together what we believe are the most reliable spectroscopic constants available for the $X^1\Sigma_g^+$ and $A^1\Sigma_u^+$ states of the ^{107,109}Ag$_2$ molecule to date, and have used them to compute potential energy curves for the two states using the Rydberg–Klein–Rees (RKR) method. We have determined the electronic transition moment function (ETMF) of the ^{107,109}Ag$_2$ $A^1\Sigma_u^+ - X^1\Sigma_g^+$ band system to be a constant value, i.e., independent of internuclear distance, and equal to 3.05 a.u. from previously reported relative absorption band strength measurements and the observed radiative lifetime of the $A^1\Sigma_u^+$ state. Based on our potential energy curves and ETMF, we have calculated, for the first time, a complete set of radiative transition parameters for the ^{107,109}Ag$_2$ $A^1\Sigma_u^+ - X^1\Sigma_g^+$ band system. The tabulated data in this paper are presented in a format that renders it readily useful to spectroscopists. We hope that these results stimulate further work toward a better understanding of electronic transitions in silver dimers. Extension of the rotational constants to higher vibrational levels and validation of the ETMF over a wider range of internuclear distances are particular areas of future interest.

Acknowledgments

This work was supported in part by the United States National Aeronautics and Space Administration, the United States National Science Foundation, and the Ministry of Science and Environmental Protection of the Republic of Serbia. The authors gratefully acknowledge Dr. Forrest R. Gilmore for several helpful suggestions for changes to the original manuscript. We also found the reviewer's comments useful and relevant. One of us (R.R.L.) also thank Dr. John Stauffer for making available discretionary support for this work at the Spitzer Science Center.

Table 3
Radiative transition parameters for the $A^1\Sigma_u^+ - X^1\Sigma_g^+$ band system of $^{107,109}\mathrm{Ag}_2$

v'	$v'' = 10$	11	12	13	14	15	16	17	18	19
0	0.4734 21123.2 4.61E−06 2.9619 8.19E+02* 2.75E−06*	0.4774 20944.9 4.25E−07 3.0080 7.36E+01* 2.51E−07*	0.4815 20767.8 3.22E−08 3.0564 5.44E+00* 1.89E−08*	0.4856 20592.0 2.14E−09 3.0933 3.52E−01* 1.24E−09*	0.4898 20417.4 1.14E−10 3.1370 1.83E−02* 6.58E−11*	0.4940 20244.1 9.27E−13 3.8675 1.45E−04* 5.30E−13*	0.4982 20072.1 1.93E−14 4.1775 2.94E−06* 1.09E−14*	0.5025 19901.3 1.08E−12 2.6935 1.60E−04* 6.05E−13*	0.5068 19731.7 7.44E−15 2.3735 1.08E−06* 4.15E−15*	0.5112 19563.5 6.56E−13 2.6604 9.26E−05* 3.63E−13*
1	0.4700 21276.7 3.05E−04 2.9255 5.54E+04* 1.84E−04*	0.4740 21098.3 3.99E−05 2.9686 7.06E+03* 2.38E−05*	0.4780 20921.2 4.21E−06 3.0137 7.27E+02* 2.49E−06*	0.4820 20745.4 3.60E−07 3.0616 6.05E+01* 2.11E−07*	0.4861 20570.8 2.49E−08 3.1127 4.08E+00* 1.45E−08*	0.4903 20397.5 1.40E−09 3.1654 2.23E−01* 8.05E−10*	0.4944 20225.5 6.31E−11 3.2221 9.83E−03* 3.60E−11*	0.4986 20054.7 1.90E−12 3.3380 2.89E−04* 1.08E−12*	0.5029 19885.2 4.60E−14 3.4448 6.82E−06* 2.58E−14*	0.5072 19716.9 1.44E−14 2.8804 2.08E−06* 8.01E−15*
2	0.4667 21429.0 6.45E−03 2.8908 1.20E+06* 3.90E−03*	0.4706 21250.6 1.24E−03 2.9321 2.25E+05* 7.45E−04*	0.4745 21073.5 1.87E−04 2.9751 3.30E+04* 1.11E−04*	0.4785 20897.7 2.23E−05 3.0204 3.84E+03* 1.32E−05*	0.4826 20723.1 2.13E−06 3.0683 3.58E+02* 1.25E−06*	0.4866 20549.8 1.64E−07 3.1183 2.68E+01* 9.52E−08*	0.4907 20377.8 1.00E−08 3.1731 1.60E+00* 5.76E−09*	0.4949 20207.0 4.50E−10 3.2542 7.00E−02* 2.57E−10*	0.4991 20037.5 1.87E−11 3.2876 2.84E−03* 1.06E−11*	0.5033 19869.2 1.74E−12 3.0498 2.57E−04* 9.75E−13*
3	0.4634 21580.1 5.25E−02 2.8579 9.95E+06 3.20E−02	0.4673 21401.7 1.60E−02 2.8975 2.96E+06 9.70E−03	0.4712 21224.7 3.63E−03 2.9387 6.54E+05* 2.18E−03*	0.4751 21048.8 6.28E−04 2.9817 1.10E+05* 3.73E−04*	0.4791 20874.3 8.46E−05 3.0270 1.45E+04* 4.99E−05*	0.4831 20701.0 8.99E−06 3.0750 1.50E+03* 5.26E−06*	0.4871 20528.9 7.57E−07 3.1262 1.23E+02* 4.39E−07*	0.4912 20358.1 5.06E−08 3.1801 8.05E+00* 2.91E−08*	0.4953 20188.6 2.63E−09 3.2416 4.09E−01* 1.50E−09*	0.4995 20020.3 9.89E−11 3.3340 1.50E−02* 5.60E−11*
4	0.4602 21730.1 1.52E−01 2.8267 2.95E+07 9.36E−02	0.4640 21551.8 8.63E−02 2.8646 1.63E+07 5.26E−02	0.4678 21374.7 3.21E−02 2.9041 5.91E+06 1.94E−02	0.4717 21198.8 8.51E−03 2.9453 1.53E+06* 5.10E−03*	0.4756 21024.3 1.68E−03 2.9884 2.95E+05* 1.00E−03*	0.4796 20851.0 2.56E−04 3.0338 4.37E+04* 1.51E−04*	0.4836 20678.9 3.01E−05 3.0817 5.02E+03* 1.76E−05*	0.4876 20508.1 2.79E−06 3.1329 4.53E+02* 1.61E−06*	0.4917 20338.6 2.01E−07 3.1885 3.19E+01* 1.16E−07*	0.4958 20170.3 1.13E−08 3.2508 1.74E+00* 6.43E−09*
5	0.4571 21879.0 9.13E−02 2.7983 1.80E+07 5.64E−02	0.4608 21700.7 1.59E−01 2.8338 3.06E+07 9.74E−02	0.4646 21523.6 1.20E−01 2.8715 2.25E+07 7.28E−02	0.4684 21347.7 5.45E−02 2.9108 9.99E+06 3.29E−02	0.4723 21173.2 1.70E−02 2.9520 3.04E+06 1.02E−02	0.4762 20999.9 3.84E−03 2.9951 6.70E+05* 2.28E−03*	0.4801 20827.8 6.54E−04 3.0405 1.11E+05* 3.85E−04*	0.4841 20657.0 8.53E−05 3.0886 1.42E+04* 4.98E−05*	0.4881 20487.5 8.63E−06 3.1400 1.40E+03* 5.00E−06*	0.4921 20319.2 6.78E−07 3.1953 1.07E+02* 3.89E−07*
6	0.4540 22026.8 1.25E−02 2.7570 2.52E+06 7.80E−03	0.4577 21848.4 3.55E−02 2.8077 6.99E+06 2.19E−02	0.4614 21671.4 1.37E−01 2.8410 2.63E+07 8.38E−02	0.4652 21495.5 1.44E−01 2.8784 2.69E+07 8.73E−02	0.4690 21321.0 8.12E−02 2.9176 1.48E+07 4.89E−02	0.4729 21147.7 2.98E−02 2.9587 5.31E+06 1.78E−02	0.4767 20975.6 7.70E−03 3.0018 1.34E+06* 4.56E−03*	0.4807 20804.8 1.47E−03 3.0473 2.49E+05* 8.64E−04*	0.4846 20635.3 2.12E−04 3.0955 3.51E+04* 1.24E−04*	0.4886 20467.0 2.34E−05 3.1470 3.78E+03* 1.35E−05*
7	0.4510 22173.5 8.28E−02 2.7382 1.70E+07 5.19E−02	0.4546 21995.2 4.97E−02 2.7688 9.97E+06 3.09E−02	0.4583 21818.1 3.73E−03 2.8281 7.31E+05* 2.30E−03*	0.4621 21642.2 9.56E−02 2.8488 1.83E+07 5.85E−02	0.4658 21467.7 1.52E−01 2.8854 2.82E+07 9.19E−02	0.4696 21294.4 1.08E−01 2.9245 1.97E+07 6.51E−02	0.4734 21122.3 4.70E−02 2.9655 8.35E+06 2.80E−02	0.4773 20951.5 1.39E−02 3.0086 2.41E+06 8.24E−03	0.4812 20782.0 2.97E−03 3.0541 5.03E+05* 1.75E−03*	0.4851 20613.7 4.73E−04 3.1024 7.81E+04* 2.76E−04*
8	0.4480 22319.1 1.28E−02 2.7006 2.68E+06 8.08E−03	0.4517 22140.8 4.41E−02 2.7471 9.02E+06 2.76E−02	0.4553 21963.7 8.08E−02 2.7773 1.61E+07 5.02E−02	0.4590 21787.9 3.88E−03 2.7956 7.56E+05* 2.39E−03*	0.4627 21613.3 5.00E−02 2.8575 9.52E+06 3.06E−02	0.4664 21440.0 1.40E−01 2.8926 2.61E+07 8.51E−02	0.4702 21268.0 1.31E−01 2.9314 2.37E+07 7.85E−02	0.4740 21097.2 6.78E−02 2.9723 1.20E+07 4.04E−02	0.4778 20927.6 2.30E−02 3.0154 3.98E+06 1.36E−02	0.4817 20759.4 5.51E−03 3.0609 9.30E+05* 3.23E−03*
9	0.4452 22463.7 4.49E−02 2.6850	0.4487 22285.4 4.57E−02 2.7123	0.4523 22108.3 9.70E−03 2.7608	0.4559 21932.4 8.61E−02 2.7854	0.4596 21757.9 2.78E−02 2.8151	0.4633 21584.6 1.52E−02 2.8697	0.4670 21412.5 1.13E−01 2.9002	0.4708 21241.7 1.44E−01 2.9384	0.4746 21072.2 9.03E−02 2.9792	0.4784 20903.9 3.53E−02 3.0222

(*continued on next page*)

Table 3 (*continued*)

v'	$v'' = 10$	11	12	13	14	15	16	17	18	19
	9.58E+06	9.53E+06	1.98E+06*	1.71E+07	5.39E+06	2.87E+06	2.10E+07	2.60E+07	1.59E+07	6.08E+06
	2.85E−02	2.88E−02	6.06E−03*	5.34E−02	1.71E−02	9.25E−03	6.86E−02	8.64E−02	5.38E−02	2.09E−02
10	0.4423	0.4459	0.4494	0.4530	0.4566	0.4602	0.4639	0.4676	0.4713	0.4751
	22607.2	22428.9	22251.8	22076.0	21901.4	21728.1	21556.1	21385.3	21215.7	21047.5
	4.84E−02	1.14E−02	6.81E−02	4.70E−04	6.56E−02	5.83E−02	3.31E−04	7.72E−02	1.45E−01	1.12E−01
	2.6537	2.6975	2.7210	2.7016	2.7937	2.8247	2.9443	2.9082	2.9456	2.9861
	1.05E+07	2.42E+06	1.41E+07	9.53E+04*	1.30E+07	1.13E+07	6.24E+04*	1.42E+07	2.61E+07	1.97E+07
	3.09E−02	7.21E−03	4.28E−02	2.93E−04*	4.06E−02	3.58E−02	2.01E−04*	4.66E−02	8.69E−02	6.66E−02
11	0.4396	0.4430	0.4465	0.4501	0.4536	0.4572	0.4609	0.4645	0.4682	0.4719
	22749.7	22571.4	22394.3	22218.5	22043.9	21870.6	21698.5	21527.8	21358.2	21190.0
	3.37E−04	6.26E−02	1.67E−04	6.42E−02	1.66E−02	3.36E−02	7.88E−02	6.57E−03	4.12E−02	1.33E−01
	2.6815	2.6623	2.6120	2.7294	2.7542	2.8032	2.8330	2.8544	2.9175	2.9529
	7.49E+04*	1.36E+07	3.54E+04*	1.33E+07	3.35E+06	6.62E+06	1.52E+07	1.24E+06*	7.56E+06	2.38E+07
	2.17E−04*	3.99E−02	1.06E−04*	4.03E−02	1.03E−02	2.08E−02	4.83E−02	4.00E−03*	2.49E−02	7.95E−02
12	0.4368	0.4403	0.4437	0.4472	0.4507	0.4543	0.4579	0.4615	0.4651	0.4688
	22891.2	22712.8	22535.7	22359.9	22185.4	22012.1	21840.0	21669.2	21499.7	21331.4
	4.52E−02	9.54E−03	4.98E−02	1.46E−02	3.99E−02	4.30E−02	7.98E−03	8.04E−02	2.75E−02	1.40E−02
	2.6082	2.6282	2.6708	2.6934	2.7384	2.7652	2.8184	2.8410	2.8706	2.9306
	1.02E+07	2.11E+06*	1.08E+07	3.08E+06	8.22E+06	8.64E+06	1.57E+06*	1.54E+07	5.16E+06	2.55E+06
	2.93E−02	6.13E−03*	3.17E−02	9.23E−03	2.50E−02	2.67E−02	4.93E−03*	4.92E−02	1.67E−02	8.41E−03
13	0.4342	0.4376	0.4410	0.4444	0.4479	0.4514	0.4549	0.4585	0.4621	0.4657
	23031.6	22853.3	22676.2	22500.4	22325.8	22152.5	21980.5	21809.7	21640.2	21471.9
	4.52E−02	1.75E−02	3.38E−02	2.32E−02	3.93E−02	1.32E−02	6.16E−02	1.16E−04	6.41E−02	5.28E−02
	2.5806	2.6184	2.6403	2.6807	2.7045	2.7504	2.7740	2.6822	2.8494	2.8804
	1.04E+07	3.94E+06	7.42E+06	4.97E+06	8.24E+06	2.71E+06	1.23E+07	2.26E+04*	1.22E+07	9.84E+06
	2.94E−02	1.13E−02	2.16E−02	1.47E−02	2.48E−02	8.27E−03	3.83E−02	7.14E−05*	3.92E−02	3.20E−02

For each $v' - v''$ band, the listed quantities are $\lambda_{v'v''}$ (μm), $\nu_{v'v''}$ (cm^{-1}), $q_{v'v''}$, $\bar{r}_{v'v''}$ (Å), $A_{v'v''}$ (spontaneous emission rate, in s^{-1}), and $f^{\mathrm{abs}}_{v'v''}$ (absorption band oscillator strength). Values of $A_{v'v''}$ and $f^{\mathrm{abs}}_{v'v''}$ having a corresponding value of $q_{v'v''} < 0.01$ are marked with an asterisk to indicate possible lower accuracy. Continuation of table on previous page.

Table 4
Radiative transition parameters for the ^{107,109}Ag$_2$ $A - X$ bands reported on by Kleman and Lindkvist [1]

Δv	$v' - v''$	$\lambda_{v'v''}$ (μm)	$\nu_{v'v''}$ (cm^{-1})	$q_{v'v''}$ (dimensionless)	$\bar{r}_{v'v''}$ (Å)	$A_{v'v''}$ (s^{-1})	$f^{\mathrm{abs}}_{v'v''}$ (dimensionless)
+5	6–1	0.4221	23689.3	1.17E−01	2.4773	2.93E+07	7.84E−02
+4	4–0	0.4240	23583.7	1.13E−01	2.4931	2.79E+07	7.53E−02
	5–1	0.4248	23541.5	1.44E−01	2.5004	3.55E+07	9.61E−02
+3	3–0	0.4267	23433.7	1.86E−01	2.5168	4.50E+07	1.23E−01
	4–1	0.4275	23392.6	1.20E−01	2.5245	2.89E+07	7.92E−02
+2	2–0	0.4295	23282.6	2.45E−01	2.5412	5.83E+07	1.61E−01
+1	1–0	0.4323	23130.3	2.32E−01	2.5664	5.42E+07	1.52E−01
	3–2	0.4338	23052.7	1.11E−01	2.5781	2.57E+07	7.26E−02
	4–3	0.4345	23014.2	9.16E−02	2.5863	2.10E+07	5.96E−02
0	0–0	0.4352	22976.8	1.18E−01	2.5924	2.71E+07	7.68E−02
	1–1	0.4359	22939.2	1.52E−01	2.5973	3.45E+07	9.82E−02
	2–2	0.4367	22901.6	1.12E−01	2.6054	2.54E+07	7.26E−02
−1	0–1	0.4389	22785.7	2.70E−01	2.6247	6.02E+07	1.74E−01
	2–3	0.4403	22713.1	1.04E−01	2.6360	2.29E+07	6.66E−02
	3–4	0.4410	22676.9	1.16E−01	2.6441	2.54E+07	7.41E−02
−2	0–2	0.4426	22595.9	2.89E−01	2.6579	6.28E+07	1.84E−01
	1–3	0.4432	22560.8	9.53E−02	2.6659	2.06E+07	6.07E−02
−3	0–3	0.4463	22407.3	1.92E−01	2.6919	4.07E+07	1.22E−01
	1–4	0.4470	22373.5	2.06E−01	2.6991	4.34E+07	1.30E−01
	2–5	0.4476	22339.8	8.99E−02	2.7070	1.89E+07	5.68E−02
−4	0–4	0.4500	22220.1	8.94E−02	2.7268	1.85E+07	5.62E−02
	1–5	0.4507	22187.5	1.77E−01	2.7337	3.65E+07	1.11E−01
	2–6	0.4514	22155.1	1.83E−01	2.7408	3.76E+07	1.15E−01
	3–7	0.4520	22122.8	1.17E−01	2.7483	2.39E+07	7.31E−02
	4–8	0.4527	22090.6	3.94E−02	2.7575	8.01E+06	2.46E−02

Table 4 (*continued*)

Δv	$v' - v''$	$\lambda_{v'v''}$ (μm)	$\nu_{v'v''}$ (cm^{-1})	$q_{v'v''}$ (dimensionless)	$\bar{r}_{v'v''}$ (Å)	$A_{v'v''}$ (s^{-1})	$f^{\text{abs}}_{v'v''}$ (dimensionless)
−5	0–5	0.4538	22034.1	3.09E−02	2.7628	6.24E+06	1.93E−02
	1–6	0.4545	22002.8	9.25E−02	2.7695	1.86E+07	5.75E−02
	2–7	0.4551	21971.6	1.51E−01	2.7763	3.02E+07	9.39E−02
	3–8	0.4558	21940.6	1.72E−01	2.7833	3.43E+07	1.07E−01
	4–9	0.4564	21909.7	1.47E−01	2.7905	2.91E+07	9.09E−02
	5–10	0.4571	21879.0	9.13E−02	2.7983	1.80E+07	5.64E−02
−6	0–6	0.4577	21849.4	8.26E−03	2.7998	1.62E+06*	5.10E−03*
	1–7	0.4583	21819.4	3.35E−02	2.8064	6.56E+06	2.07E−02
	2–8	0.4589	21789.5	7.49E−02	2.8131	1.46E+07	4.61E−02
	3–9	0.4596	21759.7	1.20E−01	2.8199	2.34E+07	7.40E−02
	4–10	0.4602	21730.1	1.52E−01	2.8267	2.95E+07	9.36E−02
	5–11	0.4608	21700.7	1.59E−01	2.8338	3.06E+07	9.74E−02
	6–12	0.4614	21671.4	1.37E−01	2.8410	2.63E+07	8.38E−02
	7–13	0.4621	21642.2	9.56E−02	2.8488	1.83E+07	5.85E−02
−7	3–10	0.4634	21580.1	5.25E−02	2.8579	9.95E+06	3.20E−02
	4–11	0.4640	21551.8	8.63E−02	2.8646	1.63E+07	5.26E−02
	5–12	0.4646	21523.6	1.20E−01	2.8715	2.25E+07	7.28E−02
	6–13	0.4652	21495.5	1.44E−01	2.8784	2.69E+07	8.73E−02
	7–14	0.4658	21467.7	1.52E−01	2.8854	2.82E+07	9.19E−02
	8–15	0.4664	21440.0	1.40E−01	2.8926	2.61E+07	8.51E−02
	9–16	0.4670	21412.5	1.13E−01	2.9002	2.10E+07	6.86E−02
	10–17	0.4676	21385.3	7.72E−02	2.9082	1.42E+07	4.66E−02
−8	5–13	0.4684	21347.7	5.45E−02	2.9108	9.99E+06	3.29E−02
	6–14	0.4690	21321.0	8.12E−02	2.9176	1.48E+07	4.89E−02
	7–15	0.4696	21294.4	1.08E−01	2.9245	1.97E+07	6.51E−02
	8–16	0.4702	21268.0	1.31E−01	2.9314	2.37E+07	7.85E−02
	9–17	0.4708	21241.7	1.44E−01	2.9384	2.60E+07	8.64E−02
	10–18	0.4713	21215.7	1.45E−01	2.9456	2.61E+07	8.69E−02
	11–19	0.4719	21190.0	1.33E−01	2.9529	2.38E+07	7.95E−02
	12–20	0.4725	21164.4	1.10E−01	2.9606	1.96E+07	6.56E−02
	13–21	0.4731	21139.1	8.00E−02	2.9687	1.42E+07	4.78E−02
−9	7–16	0.4734	21122.3	4.70E−02	2.9655	8.35E+06	2.80E−02
	8–17	0.4740	21097.2	6.78E−02	2.9723	1.20E+07	4.04E−02
	9–18	0.4746	21072.2	9.03E−02	2.9792	1.59E+07	5.38E−02
	10–19	0.4751	21047.5	1.12E−01	2.9861	1.97E+07	6.66E−02
	11–20	0.4757	21022.9	1.30E−01	2.9932	2.27E+07	7.70E−02
	12–21	0.4762	20998.6	1.41E−01	3.0003	2.45E+07	8.34E−02
	13–22	0.4768	20974.6	1.43E−01	3.0075	2.48E+07	8.46E−02
	14–23	0.4773	20950.7	1.35E−01	3.0149	2.35E+07	8.01E−02
	15–24	0.4778	20927.2	1.19E−01	3.0225	2.06E+07	7.05E−02
	16–25	0.4784	20903.9	9.66E−02	3.0305	1.66E+07	5.71E−02
	17–26	0.4789	20880.9	7.05E−02	3.0392	1.21E+07	4.16E−02
−10	10–20	0.4789	20880.4	5.07E−02	3.0291	8.70E+06	2.99E−02
	11–21	0.4795	20857.2	6.85E−02	3.0361	1.17E+07	4.04E−02
	12–22	0.4800	20834.1	8.75E−02	3.0431	1.49E+07	5.15E−02
	13–23	0.4805	20811.3	1.06E−01	3.0501	1.80E+07	6.25E−02
	14–24	0.4810	20788.7	1.23E−01	3.0572	2.08E+07	7.20E−02
	15–25	0.4815	20766.4	1.35E−01	3.0644	2.28E+07*	7.92E−02*
	16–26	0.4821	20744.3	1.41E−01	3.0717	2.38E+07	8.29E−02
	17–27	0.4826	20722.6	1.41E−01	3.0791	2.37E+07	8.27E−02
	18–28	0.4831	20701.1	1.34E−01	3.0867	2.24E+07	7.84E−02
	19–29	0.4836	20680.0	1.20E−01	3.0945	2.01E+07	7.03E−02
	20–30	0.4840	20659.1	1.02E−01	3.1027	1.69E+07	5.93E−02
	21–31	0.4845	20638.6	7.96E−02	3.1114	1.32E+07	4.64E−02
	22–32	0.4850	20618.5	5.68E−02	3.1210	9.39E+06	3.31E−02
−11	17–28	0.4863	20565.5	1.09E−01	3.1243	1.79E+07	6.35E−02
	18–29	0.4867	20545.3	1.23E−01	3.1316	2.02E+07	7.17E−02
	19–30	0.4872	20525.4	1.35E−01	3.1389	2.20E+07	7.81E−02
	20–31	0.4877	20505.8	1.42E−01	3.1464	2.30E+07	8.22E−02
	21–32	0.4881	20486.5	1.44E−01	3.1540	2.34E+07	8.34E−02
	22–33	0.4886	20467.5	1.41E−01	3.1617	2.28E+07	8.17E−02
	23–34	0.4890	20449.0	1.33E−01	3.1696	2.15E+07	7.70E−02
	24–35	0.4895	20430.7	1.21E−01	3.1777	1.94E+07	6.96E−02
	25–36	0.4899	20412.9	1.04E−01	3.1863	1.67E+07	6.01E−02

(*continued on next page*)

Tabel 4 (*continued*)

Δv	$v' - v''$	$\lambda_{v'v''}$ (μm)	$\nu_{v'v''}$ (cm^{-1})	$q_{v'v''}$ (dimensionless)	$\bar{r}_{v'v''}$ (Å)	$A_{v'v''}$ (s^{-1})	$f^{\rm abs}_{v'v''}$ (dimensionless)
	26–37	0.4903	20395.4	8.55E−02	3.1953	1.37E+07	4.93E−02
	27–38	0.4907	20378.3	6.59E−02	3.2052	1.05E+07	3.79E−02
−12	18–30	0.4904	20390.7	6.03E−02	3.1807	9.63E+06	3.47E−02
	19–31	0.4909	20372.0	7.41E−02	3.1881	1.18E+07	4.27E−02
	20–32	0.4913	20353.6	8.86E−02	3.1954	1.41E+07	5.10E−02
	21–33	0.4917	20335.6	1.03E−01	3.2028	1.63E+07	5.93E−02
	22–34	0.4922	20317.9	1.17E−01	3.2103	1.85E+07	6.71E−02
	23–35	0.4926	20300.5	1.29E−01	3.2179	2.04E+07	7.40E−02
	24–36	0.4930	20283.5	1.39E−01	3.2255	2.19E+07	7.97E−02
	25–37	0.4934	20266.9	1.46E−01	3.2332	2.29E+07	8.36E−02
	26–38	0.4938	20250.6	1.50E−01	3.2410	2.34E+07	8.57E−02
	27–39	0.4942	20234.8	1.50E−01	3.2489	2.34E+07	8.55E−02
	28–40	0.4946	20219.3	1.46E−01	3.2571	2.27E+07	8.33E−02
	29–41	0.4949	20204.3	1.38E−01	3.2654	2.15E+07	7.89E−02
	30–42	0.4953	20189.7	1.28E−01	3.2741	1.98E+07	7.28E−02
	31–43	0.4956	20175.5	1.14E−01	3.2831	1.77E+07	6.52E−02
	32–44	0.4960	20161.8	9.91E−02	3.2926	1.53E+07	5.65E−02
	33–45	0.4963	20148.6	8.29E−02	3.3029	1.28E+07	4.72E−02

For each $v' - v''$ band, the listed quantities are $\lambda_{v'v''}$ (μm), $\nu_{v'v''}$ (cm^{-1}), $q_{v'v''}$, $\bar{r}_{v'v''}$ (Å), $A_{v'v''}$ (spontaneous emission rate, in s^{-1}), and $f^{\rm abs}_{v'v''}$ (absorption band oscillator strength). Values of $A_{v'v''}$ and $f^{\rm abs}_{v'v''}$ having a corresponding value of $q_{v'v''} < 0.01$ are marked with an asterisk to indicate possible lower accuracy.

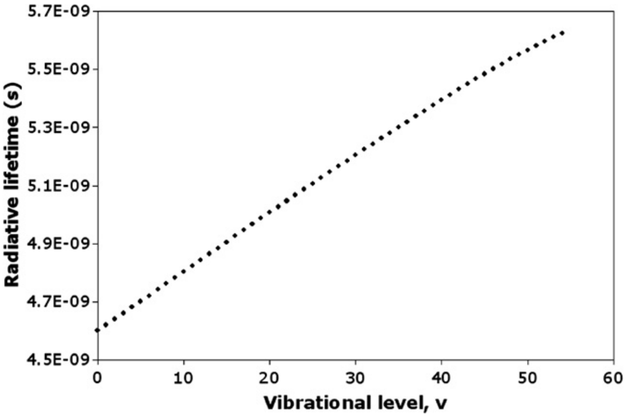

Fig. 3. Calculated radiative lifetimes of $^{107,109}\mathrm{Ag}_2\,A^1\Sigma_u^+(v)$ states.

Appendix A. Data units

We compute the leading coefficients in Eqs. (6) and (7), starting with the expressions given in Tatum's Table A5 [24]. We also include the data units of the leading coefficients (for our particular formulation), which are usually not reported alongside the often quoted values in the literature. The physical constants used in the calculations are given in Table A1. It is necessary to multiply Tatum's expressions by $a_0^2e^2$, in order to accommodate the ETMF's data units of electric dipole moment atomic units (a.u.). We also make use of the following relationship between wavelength, λ, and wavenumber, ν:

$$\frac{10^8\ \text{Å cm}^{-1}}{\lambda(\text{Å})} = \nu\ (\text{cm}^{-1}), \tag{A1}$$

Table A1
Physical constants, from Tipler [27]

Symbol	Definition	Value	Data units
h	Planck's constant	6.62618×10^{-34}	J-s
a_0	Bohr radius	5.29177×10^{-11}	m
e	Charge on electron	1.60219×10^{-19}	C
m_e	Mass of electron	9.10953×10^{-31}	kg
c	Light speed in vacuum	2.99793×10^{8}	m/s
ϵ_0	Permittivity of free space	8.85419×10^{-12}	C^2 J^{-1} m^{-1}

$$\begin{aligned} &\frac{16\pi^3}{3h\epsilon_0} \times (a_0^2e^2) \\ &\quad = \frac{16\pi^3(5.29177 \times 10^{-11})^2(1.60219 \times 10^{-19})^2}{3(6.62618 \times 10^{-34})(8.85419 \times 10^{-12})} \\ &\qquad \times (\text{a.u.})^{-2} \times (10^{10}\ \text{Å m}^{-1})^3 \times (10^8\ \text{Å cm}^{-1})^{-3} \\ &\quad = 2.026 \times 10^{-6}\ \text{cm}^3(\text{a.u.})^{-2}\ \text{s}^{-1}, \end{aligned} \tag{A2}$$

$$\begin{aligned} &\frac{8\pi^2mc}{3he^2} \times (a_0^2e^2) \\ &\quad = \frac{8\pi^2(9.10953 \times 10^{-31})(2.99793 \times 10^{8})}{3(6.62618 \times 10^{-34})} \\ &\qquad \times (5.29177 \times 10^{-11})^2 \times (\text{a.u.})^{-2} \\ &\qquad \times (10^{10}\ \text{Å m}^{-1}) \times (10^8\ \text{Å cm}^{-1})^{-1} \\ &\quad = 3.0376 \times 10^{-6}\ \text{cm}(\text{a.u.})^{-2}. \end{aligned} \tag{A3}$$

The application of Eq. (A1) in Eqs. (A2) and (A3) changes the dependence on the wavelength variable, λ (in Å), in Tatum's expressions to the dependence on wavenumber, $\nu_{v'v''}$ (in cm^{-1}), in Eqs. (6) and (7). Since Tatum's expressions require wavelength in Å, the seemingly roundabout conversion steps involving Å are included explicitly. Note that the e^2 terms in the numerator and denominator cancel in Eq. (A3).

References

[1] B. Kleman, S. Lindkvist, Arkiv för Fysik 9 (1955) 385.
[2] A. Antić-Jovanović, M. Kuzmanović, V. Bojović, M.A. Khakoo, R.R. Laher, Chinese Phys. Lett. 24 (2007) 2566.
[3] J. Ruamps, Ann. Phys. (Paris) 4 (1959) 1111.
[4] J. Ruamps, C.R. Hebd, Seances Acad. Sci. 238 (1954) 1489.
[5] C.M. Brown, M.L. Ginter, J. Mol. Spectrosc. 69 (1978) 25.
[6] R.C. Maheshwari, Ind. J. Phys. 37 (1963) 368.
[7] S.-P. Choong, L.-S. Wang, Y.-S. Lim, Nature 209 (1966) 1300.
[8] V. Beutel, H.-G. Krämer, G.L. Bhale, M. Kuhn, K. Weyers, W. Demtröder, J. Chem. Phys. 98 (1993) 2699.
[9] B. Simard, P.A. Hackett, A.M. James, P.R.R. Langridge-Smith, Chem. Phys. Lett. 186 (1991) 415.
[10] H.-G. Krämer, V. Beutel, K. Weyers, W. Demtröder, Chem. Phys. Lett. 193 (1992) 331.
[11] T. Hebert, H. Wiggenhauser, D.M. Kolb, J. Chem. Phys. 91 (1989) 1417.
[12] T. Hebert, H. Wiggenhauser, U. Schriever, D.M. Kolb, J. Chem. Phys. 92 (1990) 1575.
[13] L. König, I. Rabin, W. Schulze, G. Ertl, Science 274 (1996) 1353.
[14] I. Rabin, W. Schulze, G. Ertl, J. Chem. Phys. 108 (1998) 5137.
[15] R.W. Nicholls, W.R. Jermain, Proc. Phys. Soc. LXIX 3-A (1955) 253.
[16] R.W. Nicholls, A.L. Stewart, Atomic and Molecular Processes, Academic Press, New York, 1962.
[17] P.A. Fraser, Can. J. Phys. 32 (1954) 515.
[18] K.P. Huber, G. Herzberg, Constants of Diatomic Molecules, Van Nostrand-Reinhold, New York, 1979.
[19] M.D. Morse, Chem. Rev. 86 (1986) 1049.
[20] H. Zhang, K. Balasubramanian, J. Chem. Phys. 98 (1993) 7092.
[21] F.R. Gilmore, R.R. Laher, P.J. Espy, J. Phys. Chem. Ref. Data 21 (1992) 1005.
[22] C.O. Laux, C.H. Kruger, J. Quant. Spectrosc. Radiat. Transfer 48 (1992) 9.
[23] A. Schadee, J. Quant. Spectrosc. Radiat. Transfer 19 (1978) 451.
[24] J.B. Tatum, Astrophys. J. Suppl. 14 (1967) 21.
[25] V. Beutel, M. Kuhn, W. Demtröder, J. Mol. Spectrosc. 155 (1992) 343.
[26] G. Herzberg, Molecular Spectra and Molecular Structure, Van Nostrand-Reinhold, New York, 1955.
[27] P.A. Tipler, Modern Physics, fifth ed., Worth Publishers, Inc., 1978.